Decomposition of Formaldehyde on Cu/Ni(110) Single-Crystal Surfaces

EDWARD M. SILVERMAN AND ROBERT J. MADIX

Department of Chemical Engineering, Stanford University, Stanford, California 94305

The decomposition of formaldehyde on a clean (110)-oriented Cu/Ni single crystal was studied by flash desorption spectroscopy and Auger electron spectroscopy. The copper/nickel alloy surfaces were varied in composition from 100% Ni to 35% Ni. At 190°K formaldehyde appeared to adsorb dissociatively to form $H_{(a)}$ and $CO_{(a)}$. The desorption of CO was first order while the desorption of H_2 obeyed complex kinetics. The H_2 and CO production from H_2CO decreased with increasing surface copper content. This effect was due to the requirement of a cluster of two nickel atoms on the surface to decompose the formaldehyde molecule. The possible stabilization of an H–CO surface intermediate on the Cu-rich surfaces is discussed.

I. INTRODUCTION

The major interest of alloying in the field of catalysis is the effect it can produce on the selectivity and the activity for catalytic reactions. Recently the behavior of alloy surfaces has been interpreted in terms of both ligand effects and the requirement of active metal atoms clusters for adsorption or product formation (1). Previous studies by Yu et al. (2) on the thermal desorption of CO and H_2 and by Ying and Madix (3) on the flash decomposition of formic acid from a clean (110)-oriented copper/nickel alloy single crystal have illustrated the relative importance of ligand and cluster effects in the surface reactivity of alloys. In order to examine the interplay between these two effects further, and to delineate the cluster size needed to decompose other molecules, the decomposition of formaldehyde was studied on the same copper/nickel alloy single crystal.

II. EXPERIMENTAL METHODS

Temperature-programmed reaction spectroscopy (TPRS) was used to study the decomposition of H_2CO on clean Cu/Ni alloy surfaces. The stainless-steel ion-pumped ultra-high vacuum chamber used was described previously (4). Briefly, it contained an EAI quadrupole mass spectrometer and PHI four-grid Auger-LEED optics. A base pressure of 1×10^{-10} Torr was routinely reached. The formaldehyde was introduced onto the alloy surface through a stainless-steel dosing syringe directed at the front face of the crystal.

The Cu/Ni alloy sample studied was a (110)-oriented single-crystal whose bulk atomic composition was 10% Cu–90% Ni. A detailed description of the method of preparation was given elsewhere (5–7). Alloy surface compositions ranging from 87% Ni/13% Cu to 35% Ni/65% Cu were obtained from the sample by different annealing schedules subsequent to ion
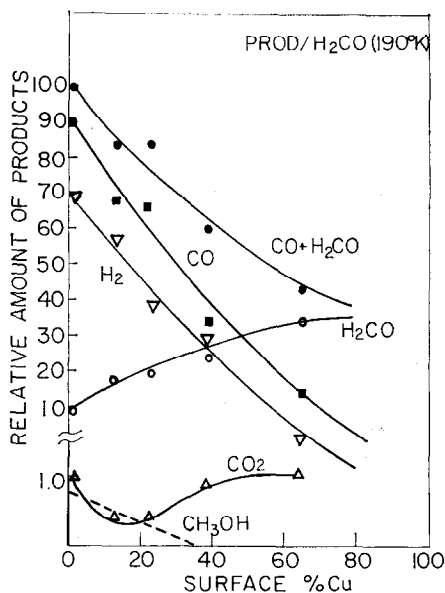
FIG. 1. Plot of relative amount of products of the H_2CO decomposition versus Cu surface concentration (exposure = 10 Langmuir).

bombardment. In general the alloy surface was copper enriched after annealing because of segregation of copper atoms to the surface, as predicted by several surface segregation models (8–10). Utilizing the fact that Cu diffuses quite slowly in the bulk of the alloy (11), while at the surface the diffusion process is much faster (12), the amount of copper segregation could be controlled by varying the annealing temperature (704–904°K). Since Cu was sputtered preferentially from the alloy surface (12), a surface composition of approximately 100% Ni was easily obtained on a sputtered surface. Auger electron spectroscopy (AES) was used to determine the alloy surface composition, and the details are published elsewhere (2, 3, 14). The surface compositions achieved were quite reproducible if the same technique was followed. Furthermore, the adsorption and thermal desorption of H_2CO did not change the surface composition, as confirmed by auger measurements before and after desorption.

LEED studies gave evidence that an-

nealing was able to repair the surface damages induced by sputtering and to regenerate the surface crystallinity. On the sputtered surface, only a diffuse pattern was observed. However, the LEED spectrum of an annealed surface, even at the lowest annealing temperature used, showed sharp (1 × 1) spots.

The surface of the sample was cleaned by repetitive cycles of argon ion sputtering and heating. AES was used to monitor the degree of surface contamination. Carbon was very difficult to remove completely, as somewhat less than 10% of a surface carbon monolayer was always present after ion bombardment. However, annealing the sample at high temperatures (>827°K) for 5 min resulted in an elimination of any detectable surface carbon for the copper-rich surface.

III. RESULTS: FLASH DECOMPOSITION OF H_2CO

For all the alloy surfaces studied formaldehyde was readily adsorbed at 190°K. On the 100% Ni sputtered surface, the major desorbing species were H_2 and CO with small amounts of CH_3OH, CO_2, and unreacted H_2CO. With increasing Cu concentration the formation of CO, H_2, and CH_3OH decreased while the desorption of unreacted H_2CO increased, as shown in Fig. 1. A steady decrease was observed in the total H_2CO adsorption with increasing Cu concentration. No other flash decomposition products were observed on any of the Cu/Ni alloy surfaces. In particular, methane, water, methyl formate, methyl ether, and ethanol were all absent from the desorption spectra. When differences in mass spectrometer sensitivities and pumping speeds were corrected for, a 10 Langmuirs exposure of H_2CO resulted in an H_2:CO ratio in the products approaching 0.90 ± 0.15 for most of the alloy surfaces, indicating a stoichiometric balance to within experimental error.

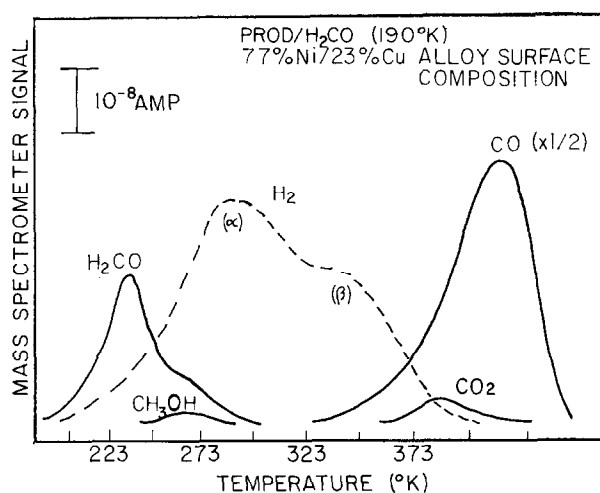Typical flash spectra for the decom-

FIG. 2. Flash decomposition spectra following H_2CO adsorption at 190°K on a 77% Ni/23% Cu surface. The H_2CO exposure was 10 Langmuir. The heating rate was 13°K/sec.

position products are shown in Fig. 2 and Fig. 3 for an Ni-rich surface and a Cu-rich surface, respectively. For high coverages of formaldehyde on the Cu-rich surface, three hydrogen desorption peaks were observed. These peaks are hereafter referred to as the α, β, and γ peaks.

For the Ni-rich alloy surfaces, the α- and β-H_2 peak positions remained essentially the same (see Table 1), with varying surface composition, though the magnitudes of both peaks decreased uniformly with increasing Cu-concentration. On the Cu-rich surface (35% Ni), the α- and β-H_2 desorption peaks shifted to higher temperatures. The γ-H_2 desorption peak, hardly detected on the Ni-rich surfaces, was more discernible on the 35% Ni surface and nearly coincided with the high temperature CO peak (see Fig. 3).

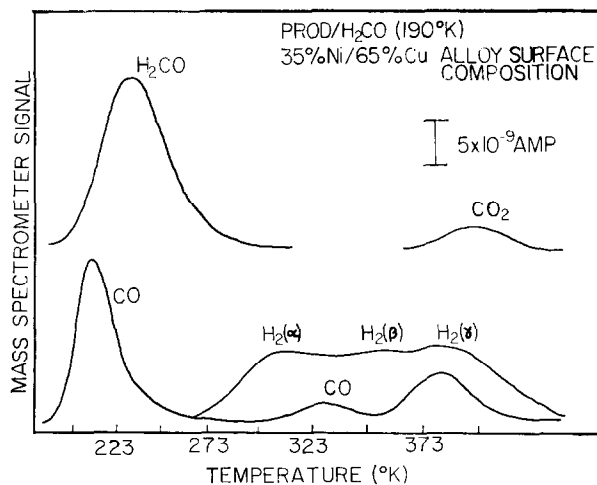An H_2 spectrum taken subsequent to the adsorption of H_2CO at low tempera-

FIG. 3. Flash decomposition spectra following H_2CO adsorption at 190°K on a 35% Ni/65% Cu surface. The H_2CO exposure was 10 Langmuir. The heating rate was 13°K/sec.

TABLE 1

Peak Positions for the Decomposition Products for the Formaldehyde Reaction[a]

	Ni(100)	Sputtered surface	87% Ni	77% Ni	61% Ni	35% Ni	Cu(110)
$H_2(\alpha)$	290°K	301	291	293	288	314	[b]
$H_2(\beta)$	364[c]	365[c]	—[d]	364[c]	364[c]	356	364
$H_2(\gamma)$	[b]	[b]	[b]	412	404	387	[b]
CO	439	423	423	423	220	220	[b]
					410	340	
						388	
CO_2	369	363	386	388	387	401	477
H_2CO	237	234	241	238	231	239	229

[a] Exposure = 10 Langmuir.
[b] Product was not detected.
[c] Room temperature adsorption.
[d] Not examined.

tures on a 77% Ni/23% Cu surface is shown as a function of formaldehyde exposure in Fig. 4. The β-H_2 peak could be isolated by adsorbing H_2CO at room temperature. An isotherm analysis (17) yielded a desorption order near two for this peak (see Fig. 5). This suggested that the H-atom recombination process was approximately second order, but the observation that the α- and β-H_2 peak temperatures were invariant with coverage indicated more complex kinetics. This

results is in agreement with previous studies (2, 4, 15, 16).

The activation energies for the β-hydrogens peaks were determined by changing the heating rate and noticing the shift in peak temperatures. For three different Cu/Ni alloy surfaces (100% Ni, 77% Ni, 61% Ni), an average activation energy value of 23.8 ± 0.7 kcal/mole was obtained.

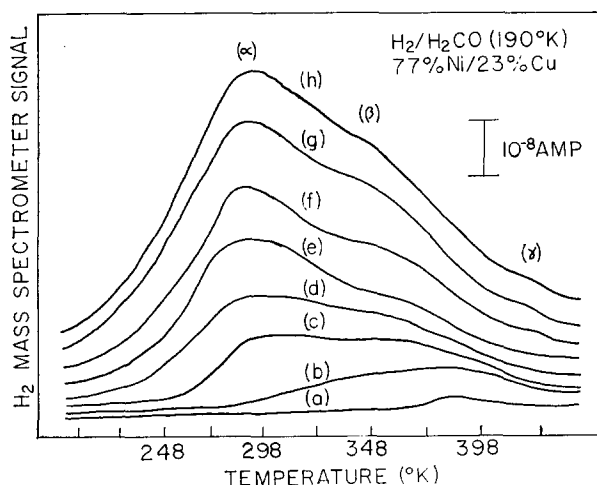For all the alloy surfaces the high temperature CO peak exhibited first-order desorption behavior and was desorption

FIG. 4. H_2 product flash desorption spectra as a function of H_2CO exposure on a 77% Ni/23% Cu surface. H_2CO adsorption was at 190°K. The H_2CO exposures were: (a) 0.1 L, (b) 0.2 L, (c) 0.5 L, (d) 1.0 L, (e) 2.5 L, (f) 5.0 L, (g) 10.0 L, (h) 20.0 L. The heating rate was 13°K/sec.

limited. On the Cu-rich surface the appearance of two additional CO peaks, located at 220 and 340°K, was observed. Both peaks corresponded to desorption states of CO on this alloy (2). For all alloy surfaces the CO_2 peak exhibited first-order desorption.

As the H_2CO decomposition reaction proceeded readily on Ni and hardly at all on Cu (see below), it was reasonable to assume that the active sites for decomposition involved a cluster of nickel atoms. The concentration of the active groups of n nickel atoms at the surface was given by:

$$X_s \alpha (X_{Ni})^n$$

where

X_s = concentration of surface sites which were catalytically active,

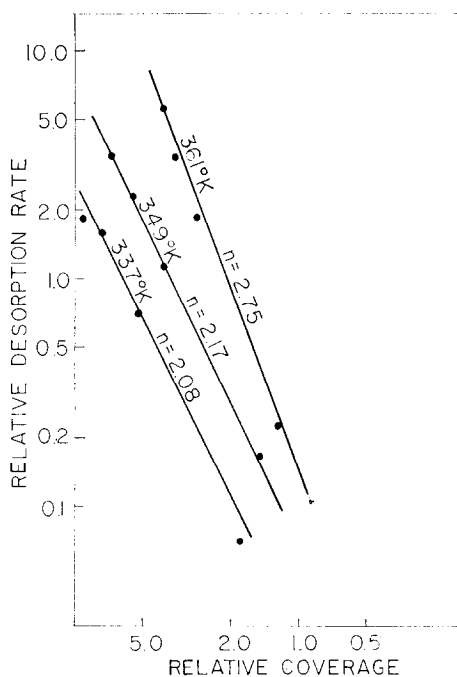X_{Ni} = concentration of nickel on the surface,

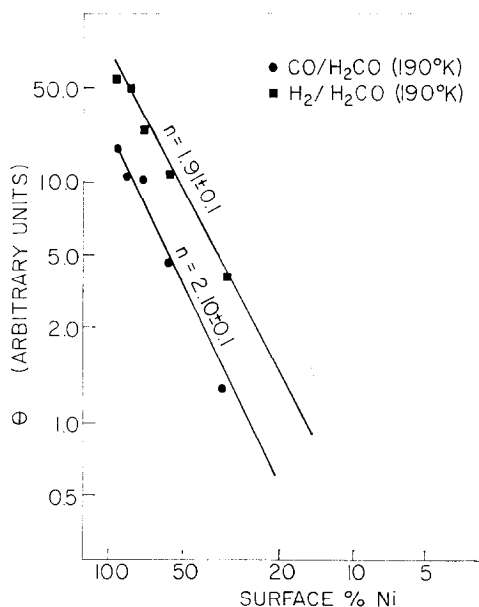n = site coordination number.

FIG. 6. ln–ln plot of H_2 product and CO product versus the nickel surface fraction: θCO = CO product, θH_2 = H_2 product, X_{Ni} = nickel surface fraction, H_2CO exposure = 10 Langmuir.

Since the decomposition rate has the following form:

$$\text{rate} = \frac{-d[H_2CO]}{dt} = \frac{d[CO]}{dt} = \frac{d[H_2]}{dt}$$
$$= X_s e^{-E/RT},$$

the overall reaction rate can be expressed as

$$\text{rate} = (X_{Ni})^n e^{-E/RT}.$$

From the above equation a ln–ln plot of the amount of CO produced at saturation coverage versus nickel surface composition yielded a straight line with slope n. This particular analysis was performed for the CO and H_2 desorption peaks as shown in Fig. 6. The amount of each product formed (area under the thermal desorption curve) was found to be proportional to the second power of surface Ni concentration.
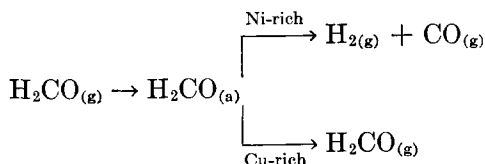

FIG. 5. Isothermal desorption rates for H_2 desorption from the 100% Ni sputtered alloy. T_{ads} = 300°K.

IV. DISCUSSION

A. Alloy Effects on Reaction Pathway

Previous work has shown the reactivity of H_2CO to differ greatly on pure nickel

or copper. On clean Ni(110) Dickinson and Madix (18) found the major reaction products to be H_2 and CO with considerable amounts of CH_3OH, CO_2, and unreacted H_2CO. However, on a Cu(110) surface H_2CO was found not to produce CO, and unreacted H_2CO comprised over 95% of the total gases desorbing from the surface (19); the remainder consisted of H_2 and CO_2.

The above conclusions fit well with the results shown in Fig. 1, in which a decrease in the H_2 and CO production was accompanied by a steady rise in the amount of unreacted H_2CO desorbing from the surface. Hence, alloying nickel with copper dramatically changed the probability for H_2CO decomposition as shown by the following reaction schematic:
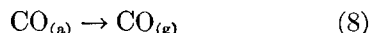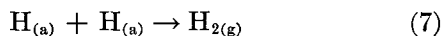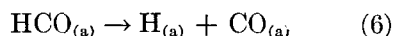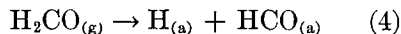
$$H_2CO_{(g)} \rightarrow H_2CO_{(a)} \begin{array}{c} \xrightarrow{\text{Ni-rich}} H_{2(g)} + CO_{(g)} \\ \\ \xrightarrow[\text{Cu-rich}]{} H_2CO_{(g)} \end{array}$$
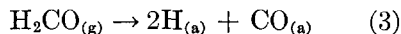
B. Kinetics of H_2CO Decomposition on Cu/Ni Alloys

1. Mechanism. The following experimental evidence supports a model of low-temperature dissociative adsorption of H_2CO to yield $H_{(a)}$ and $CO_{(a)}$:

(a) The appearance of two second-order H_2 desorption peaks, nearly identical to those observed following H_2 adsorption;
(b) The relatively small H_2CO desorption signal detected from the 100% Ni surface. (The increase in the H_2CO desorption signal with increasing Cu concentration was probably due to the adsorption of formaldehyde on Cu sites which was shown (19) to be inactive for H_2CO decomposition);
(c) The small amount of CH_3OH which was formed.

Hence, the following mechanism is proposed:

$$H_2CO_{(g)} \rightarrow H_2CO_{(a)} \quad (1)$$

$$H_2CO_{(a)} \rightarrow H_2CO_{(g)} \quad (2)$$

$$H_2CO_{(g)} \rightarrow 2H_{(a)} + CO_{(a)} \quad (3)$$

$$H_2CO_{(g)} \rightarrow H_{(a)} + HCO_{(a)} \quad (4)$$

$$H_{(a)} \rightarrow H_{2(g)} \quad (5)$$

$$HCO_{(a)} \rightarrow H_{(a)} + CO_{(a)} \quad (6)$$

$$H_{(a)} + H_{(a)} \rightarrow H_{2(g)} \quad (7)$$

$$CO_{(a)} \rightarrow CO_{(g)} \quad (8)$$

Steps (4) and (6) are indicated by the γ-H_2 peak, which desorbs at the same temperature as the high temperature CO desorption peak (see Fig. 3), well above that normally expected if H_2 desorption from the surface were the rate limiting step. In all previous work on H_2 desorption from Ni, Cu, and Cu/Ni surfaces, no H_2 binding state is known to exist at this particular temperature. Additionally, this γ-H_2 desorption peak is at a lower temperature than the CO_2 desorption peak, and there was two times as much H_2 produced as CO_2, which rules out the possibility of the γ-H_2 peak resulting from the decomposition of a surface formate. Since this H_2 peak coincided with the high temperature CO desorption peak, it appeared that a surface intermediate of the form H–CO was produced due to the relative isolation of nickel atoms on the copper-rich alloy surface.

2. Desorption of CO. When our results were compared with the CO desorption work of Yu et al. (2) on the Cu/Ni alloys, it was concluded that the lowest temperature desorption peak at 220°K was associated with desorption from a pure Cu site, the peak at 340°K with desorption from a Cu–Ni site, and the highest temperature peak with desorption from a pure Ni site. However, whereas Yu et al. observed the low temperature CO peaks on

the Ni-rich surfaces, in the present study these CO peaks were only observed on the Cu-rich surfaces. A plausible explanation of this difference is that, since H_2CO only dissociated on Ni sites, one would expect to see CO desorption primarily from Ni sites. However, at higher Cu concentration, there is a greater availability of Cu sites bordering Ni clusters so that the CO can desorb from Cu and Cu–Ni sites. These results indicate that the mobility of bound CO is not appreciable at these temperatures.

3. Desorption of CH₃OH. Methanol desorbed from the Cu/Ni surface at 265°K, the same temperature at which CH_3OH desorption subsequent to H_2CO adsorption on Ni(110) was observed (*18*). The methane desorbed from the sputtered surface contributed only 0.6% of the total reaction products, considerably less than the amount of methane (5.6%) desorbed from the Ni(110) surface. Dickinson and Madix (*18*) concluded that there existed a minimum exposure for methanol production and suggested the proximity of two surface formaldehyde molecules as a necessary condition for the production of methanol. Hence, the following mechanism was offered:

$$2H_2CO_{(a)} \rightarrow CH_3O_{(a)} + HCO_{(a)}$$

$$CH_3O_{(a)} + H_{(a)} \rightarrow CH_3OH_{(g)}$$
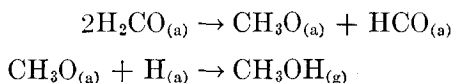
The $HCO_{(a)}$ could then further react to form the CO_2 producing intermediate HCOO or decompose to $H_{(a)}$ and $CO_{(a)}$. The reduced amount of CH_3OH formed on the 100% Ni sputtered surface indicated this reaction was structure sensitive.

4. Desorption of H₂CO. The H_2CO peak temperature was identical for the Ni(110) surface, the sputtered surface (100% Ni), the Cu/Ni alloy surfaces, and the Cu(110) surface. However, according to Fig. 1, there was a steady decrease in the total H_2CO adsorption with increasing Cu concentration, contrary to what one would normally expect if the number of available sites for gas adsorption was assumed to remain constant for all the alloy surfaces. A possible explanation for this discrepancy was that H_2CO was not adsorbed to its saturation value. However since the amount of H_2 formed did reach a saturation value, it is postulated that H_2CO was preferentially adsorbed on the Ni sites where decomposition occurred, as opposed to the Cu sites which were inactive for decomposition. Consequently, for the Cu-rich surfaces, empty Cu sites were still available for the adsorption of H_2CO. A valid argument for the above deduction is that the initial relative sticking probability of $(CO + H_2CO)$ for the 100% Ni, 87% Ni, and 77%Ni surfaces has approximately the same value. These results also indicate the existence of a precursor state for the dissociative adsorption of H_2CO.

C. Activation Energies

The activation energy for hydrogen desorption from Ni, Cu, and Cu/Ni alloy surfaces was reported in the literature by several investigators (*2, 14, 15*). Falconer and Madix calculated an activation energy of 25 kcal/mole on a single-crystal Ni(110) sample. For low coverages on a Ni(110) surface, Lapujoulade and Neil obtained an activation energy of 20.3 kcal/mole. Using a Cu/Ni(110) sample, Yu *et al.* obtained an average activation energy of 18.5 ± 0.7 kcal/mole for the 82% Ni/ 18% Cu, 65% Ni/35% Cu, and 52% Ni/ 48% Cu alloy surfaces. From the formaldehyde results an activation energy value of 23.8 ± 0.7 kcal/mole was obtained from the 100% Ni, 77% Ni/23% Cu, and 61% Ni/39% Cu surfaces. The consistency of the activation energy values with varying surface composition suggests that the surface composition does not have an appreciable effect on the activation energy of desorption for H_2.

D. *Ligand vs Cluster Effect*

The importance of the cluster requirement in the decomposition activity of the Cu/Ni alloy surfaces is clearly revealed in this study. As previously mentioned, a decrease in the decomposition reactivity was observed with increasing Cu-rich surfaces. Due to the inactivity of the Cu(110) surface for the H_2CO decomposition reaction, this result was associated with the decrease in the number of active nickel sites. Since the CO and H_2 production was proportional to the second power of surface Ni concentration, it is concluded that the decomposition reaction required two nickel sites (excluding any possibility of mixed sites, i.e., Cu/Ni).

Ligand effects seem to be secondary to the cluster requirement as a spread of only ±0.7 kcal/mole in the activation energies was calculated for the above Cu/Ni surfaces. However, as noted in Table 1, there was a downward shift in the high temperature CO peak position on the Cu-rich surfaces, which indicates a weakening of the metal-CO bond. This shift in CO peak position with surface composition has also been reported by Ertl and Kuppers (*20*) and by Yu *et al.* (*2*). Hence, there seems to be present a weak ligand effect of copper to the surface nickel atoms of this alloy.

V. SUMMARY

At 190°K formaldehyde is adsorbed dissociatively to $H_{(a)}$ and $CO_{(a)}$ on the copper/nickel alloy surfaces. The decrease in the CO and H_2 production was proportional to the second power of surface Ni concentration, leading to the conclusion that a cluster of two nickel atoms was necessary for the decomposition of a H_2CO molecule. Consequently, the results of the present study clearly revealed that the major effect of alloying was the dilution

of active sites, as ligand effects were found to be secondary to the cluster requirement in the surface reactivity of this alloy. In addition, on the Cu-rich surfaces, the observation of a γ-H_2 state, which did not appear in previous thermal desorption studies of H_2 (*2, 4, 15, 16*), was evidence that an H–CO surface intermediate may have been stabilized.

REFERENCES

1. (a) Verbeck, H., and Sachtler, W. M. H., *J. Catal.* **42**, 257 (1976); (b) Ponec, V., *Catal. Rev.-Sci. Eng.* **11**, 1 (1975); (c) Sinfelt, J. H., Carter, J. L., and Yates, D. J. C., *J. Catal.* **24**, 283 (1972); (d) Ponec, V., and Sachtler, W. M. H., *J. Catal.* **24**, 250 (1972); (e) Sachtler, W. M. H., and Doriego, G. V. H., *J. Catal.* **32**, 315 (1974).
2. Yu, K. Y., Ling, D. T., and Spicer, W. E., *J. Catal.* **44**, 373 (1976).
3. Ying, D. H. S., and Madix, R. J., to be published.
4. Falconer, J. L., and Madix, R. J., *J. Catal.* **30**, 235 (1973).
5. Helms, C. R., *J. Catal.* **35**, 114 (1975).
6. Helms, C. R., and Yu, K. Y., *J. Vac. Sci. Tech.* **12**, 276 (1975).
7. Helms, C. R., Yu, K. Y., and Spicer, W. E., *Surface Sci.* **52**, 217 (1975).
8. van Santen, R. A., and Boersma, M. A. M., *J. Catal.* **34**, 13 (1974).
9. (a) Williams, F. L., and Boudart, M., *J. Catal.* **30**, 438 (1973); (b) Williams, F. L., and Nason, P., *Surface Sci.* **45**, 377 (1974).
10. Burton, J. J., and Hyman, E. A., *J. Catal.* **37**, 114 (1975).
11. Moss, S. C., *Phys. Rev. Lett.* **23**, 38 (1969).
12. Buytymowicz, D. R., Manning, J. R., and

Reed, M. E., *J. Phys. Chem. Ref. Data* **2**, 643, (1973).

13. Turng, M. L., and Wehner, G. K., *J. Appl. Phys.* **42**, 2449 (1971).

14. Helms, C. R., *J. Catal.* **36**, 114 (1975).

15. Lapuyoulade, J., and Neil, K. S., *J. Chem. Phys.* **70**, 5 (1973).

16. Christmann, K., Schober, O., Ertl, G., and Neamann, M., *J. Chem. Phys.* **60**, 4528 (1974).

17. Falconer, J. L., and Madix, R. J., *J. Catal.* **48**, 262 (1977).

18. Dickinson, J. T., and Madix, R. J., *Int. J. Chem. Kinet.*, in press.

19. Wachs, I. E., and Madix, R. J., to be published.

20. Ertl, G., and Kuppers, J., *J. Vac. Sci. Tech.* **9**, 829 (1971).